ISTITUTO NAZIONALE DI FISICA NUCLEARE
Laboratori Nazionali di Frascati

LNF-86/31(P)
25 Luglio 1986

G. Pancheri and Y.N. Srivastava:

QCD JETS: A PERTURBATIVE APPROACH TO LOW-p_t PHYSICS

Talk given at the Workshop on Physics Simulations at High Energy
Madison, Wisconsin, May 5-16 (1986)

Servizio Documentazione
dei Laboratori Nazionali di Frascati
Cas. Postale 13 - Frascati (Roma)

INFN - Laboratori Nazionali di Frascati
Servizio Documentazione

LNF-86/31(P)
25 Luglio 1986

QCD JETS: A PERTURBATIVE APPROACH TO LOW-p_t PHYSICS(*)

G. Pancheri
INFN - Laboratori Nazionali di Frascati, P.O.Box 13, 00044 Frascati (Italy)(°)
and High Energy Physics Laboratory, Harvard University, Cambridge, 02138 Massachusetts

and

Y.N. Srivastava
Northeastern University, Boston, Massachusetts 02115
and Physics Department, University of Perugia, Perugia (Italy)

ABSTRACT

The contribution of QCD Jets to the rise with energy of the inelastic cross-section is discussed quantitatively and found to be large. It is seenthat the inclusive jet yield is the fastest growing component of the total cross-section. The dependence of this yield upon the rapidity cuts, the choice of parton densities, the QCD scale Q^2 and the transverse momentum cutoff p_0 are examined. At higher energies, multiple parton scattering processes are seen to be non-negligible. Extrapolations of the jet yield to the Tevatron and beyond are also presented.

(*) Supported in
(°) Permanent Address

1. - INTRODUCTION

In this lecture we discuss the contribution of QCD processes to the observed rise with energy of the inelastic non-single diffractive cross-section. Although QCD is believed to be the fundamental theory of strong interactions, very little effort has been dedicated so far to establish the connection between large cross-section phenomena, i.e. the hadronic multiplicity distribution and the like, and the high p_t jet phenomenon well explained by QCD calculations. Recently such a connection has been advocatedto explain a variety of anomalies which have been observed in the total inelastic cross-section as the energy increased from FNAL, through the ISR up to the S$\bar{p}$p S Collider[1-10]. Among these so called low-p_t anomalies are :

(i) the rise of the plateau, i.e. the logarithmic increase with energy of the number of particles per unit of rapidity, emitted at 90 ° in the laboratory frame. This phenomenon violates Feymann scaling which predicts a constant value for the height of the plateau.

(ii) the growth of $< p_t >$ with multiplicity, i.e. the fact that single particle transverse momentum distributions are flatter in high multiplicity samples[1]. This phenomenon, first observed in cosmic rays[2] was confirmed at the Cern Collider, and found to be present, albeit to a lesser extent, also in the ISR data at 63 GeV[3].

(iii) KNO scaling violations, which imply increasing fluctuations around the mean value, in the number of emitted particles[4].

(iv) rise of the total hadronic cross-sections, pp, $\bar{p}$p and πp[5].

Independent explanations for each of the above phenomena have been put forward, but we believe that they collectively signal the presence of an increasing contribution of hard parton-parton collisions in hadronic scattering. The physical mechanism is rather simple : as the hadronic cms energy increases, more and more partons of given energy $\frac{\sqrt{\hat{s}}}{2}$ can be produced. More precisely, since the density of gluons is more peaked at small x than that of quarks, a copious production of semi-hard gluons starts to take place. Then, if $\frac{\sqrt{\hat{s}}}{2}$ is large enough so that $\alpha_s(\hat{s})$ is small, a hard scattering process initiates which can be described by a first order QCD calculation, eventually accompanied by higher order QCD corrections.

The properties of particles produced in these QCD processes are believed to be different from those produced in the bulk of soft non-perturbative process. In particular, both their distribution in space as well as their energy-momentum properties are different. Since hard scattering is characterized by more central production (relative to the rest of the event) we can expect that as the energy increases the central region receives an increasing contribution from particles produced in a jet event. Thus the logarithmic rise with energy of the central plateau can be understood as due to QCD jets provided the jet cross-section is large enough and with the proper energy dependence. We shall see that this is indeed the case. As for KNO scaling violations and the growth of $< p_t >$ with multiplicity, it is easy to see that there is a correlation between the two effects if jet events are characterized by higher multiplicity and a higher $< p_t >$ than the no-jet sample. Qualitatively the higher $< p_t >$ value for jet events reflects the smaller average distance at which the scattering occurs. Similarly the larger number of emitted particles can be ascribed to a greater inelasticity, but also to the details of the QCD processes, like the dominance of gluon-gluon scattering which implies different color factors in the particle production mechanism. A full quantitative QCD calculation of these effects is still not possible, because inclusive particle distributions require knowledge not only of the perturbative process, but also of

the dynamics of the underlying event. A useful approach, however limited in predictive power, is to write for the inclusive cross-section

$$d\sigma = d\sigma^{NP} + d\sigma^{QCD} \tag{1}$$

where $d\sigma^{QCD}$ represent that part of the cross-section which receives contribution from processes which can be satisfactorily calculated using first order QCD. What one can calculate is the total integrated jet yield relative to the inelastic cross-section and see if such yield adequately accounts for the various anomalies discussed at the beginning. To be specific, a first estimate of KNO scaling violations requires the second term in eq.(1) to be $\approx$ 10% of the first one at 546 GeV. At first sight this number appears too high. The jet phenomenon in the past has been measured selecting events where at least one jet is produced in the central region with transverse momentum $E_T \geq 20\ GeV$ and comparing angular and transverse momentum distributions with QCD predictions. With such cuts in E_T, the jet yield is no more than a few per mille of the total inelastic cross-section. On the other hand the sharp rise of QCD cross-sections at small E_T predicts that by lowering the jet detection threshold the jet yield should sharply rise and also that for any given E_T value, the jet production rate is fast growing function of $\sqrt{s}$. The question then arises as to how low in E_T the jet phenomenon, as described by perturbative QCD, would persist. Recently the UA1 collaboration has launched a search for low-E_T jets in the minimum bias data sample at $\sqrt{s} = 546$ and 630 GeV and subsequently performed the same analysis during the ramping run, thus measuring the energy dependence of the low-E_T jet yield and associated quantities. With a nominal jet threshold at 5 GeV , the yield at 546 GeV was measured to be $\approx$ 15% of the inelastic cross-section, thus confirming the presence of a large number of jets in the minimum bias data sample. In this paper, we will compare the theoretical QCD predictions with the results of this analysis as recently reported by UA1, starting with the inclusive jet transverse momentum distribution up to the total jet cross-section. These calculations should help clarify the role played by low-E_t jets in the observed rise with energy of the inelastic non-single diffractive cross-section.

2. - DIFFERENTIAL JET DISTRIBUTIONS

The total cross section consists of various components, which can be schematically indicated as *elastic*, *single diffractive* and *inelastic* (including in the latter also the double diffractive part). An inspection of the data shows the following general trends :

(i) the elastic cross-section σ_{el} increases with energy [5],

(ii) the single diffractive cross-section remains approximately constant[11],

(iii) while $\sigma_{sd} \approx \sigma_{el}$ at the ISR, we have $\sigma_{sd} \approx 0.6\sigma_{el}$ at the Cern Collider.

(iv) the ratio $\frac{\sigma_{el}+\sigma_{sd}}{\sigma_{tot}}$ remains practically constant and $\approx \frac{1}{3}\sigma_{tot}$ from FNAL energies through the ISR and up to the CERN Collider. We illustrate this in **Fig.1**, where we show the quantity $\sigma_{tot} - \sigma_{el} - \sigma_{sd}$ as a function of $\sqrt{s}$ and compare it with the expression for $\frac{2}{3}\sigma_{tot}$ obtained from the well known fit by Amaldi et al.[12].

(v) the jet cross-section as measured by UA1 rises faster than any other component. This can also be seen from **Fig.1** where we have plotted the UA1 minimum bias jet data[13].

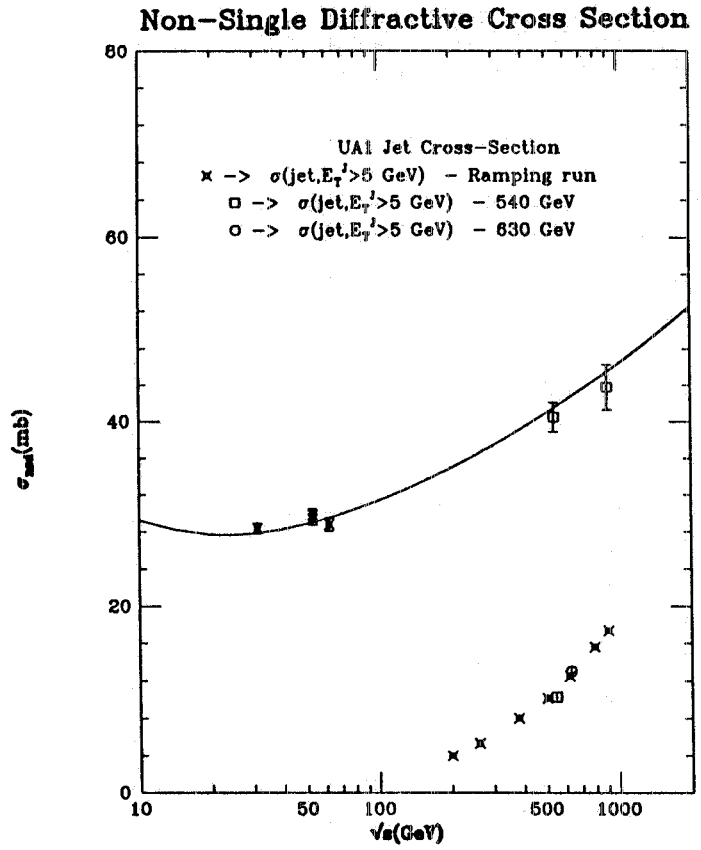

Fig.1 : Experimental data (from the review in ref.5) for $\sigma_{ned} = (\sigma_{tot} - \sigma_{el} - \sigma_{sd})$ vs. $\sqrt{s}$ are shown alongwith the continuous curve for $\frac{2}{3}\sigma_{tot}$ obtained from ref.12. Also shown are the preliminary UA1 data for the inclusive jet yield from ref.13.

To investigate the role played by QCD processes in the rise of the total cross-section we start by recalling the main features of the jet phenomenon as observed at IRS and at the Cern Collider. For very large transverse energies, the jet phenomenon is rather spectacular[14,15]. Its kinematics is well understood by QCD predictions, as reflected in the two jet-angular distribution[16]. The transverse energy cross-sections are well described by QCD calculations and structure functions which are extrapolated in Q^2 from neutrino scattering data . In Figs. 2a) and b), we show the first order QCD predictions for the differential cross-section for inclusive jet production as a function of the jet transverse momentum at different energies, at 90° in the proton-antiproton c.m.,down to $E_T \geq 5\ GeV$. The solid curves are obtained from the expression

$$\frac{d\sigma}{d\eta dp_t} = \frac{\pi}{2{p_t}^3}\int_{x_{10}}^{1}\frac{F(x_1)}{x_1^2}\frac{F(x_2)}{x_2^2}\alpha_s(Q^2)^2\frac{x_T^4}{(2x_1 - x_T e^{\eta})}|A|^2 \qquad (2a)$$

where $x_2 = \frac{x_1 x_T e^{-\eta}}{(2x_1 - x_T e^{\eta})}$, $x_{10} = \frac{x_T e^{\eta}}{(2 - x_T e^{-\eta})}$, $x_T = \frac{2p_t}{\sqrt{s}} = \sqrt{x_1 x_2}\sin\theta^*$ and the c.m. scattering angle θ^* satisfies

$$z^* = \cos\theta^* = \frac{(x_1 e^{-\eta} - x_2 e^{\eta})}{(x_1 e^{-\eta} + x_2 e^{\eta})}$$

In the small angle limit, all amplitudes can be approximated by the same term, viz.

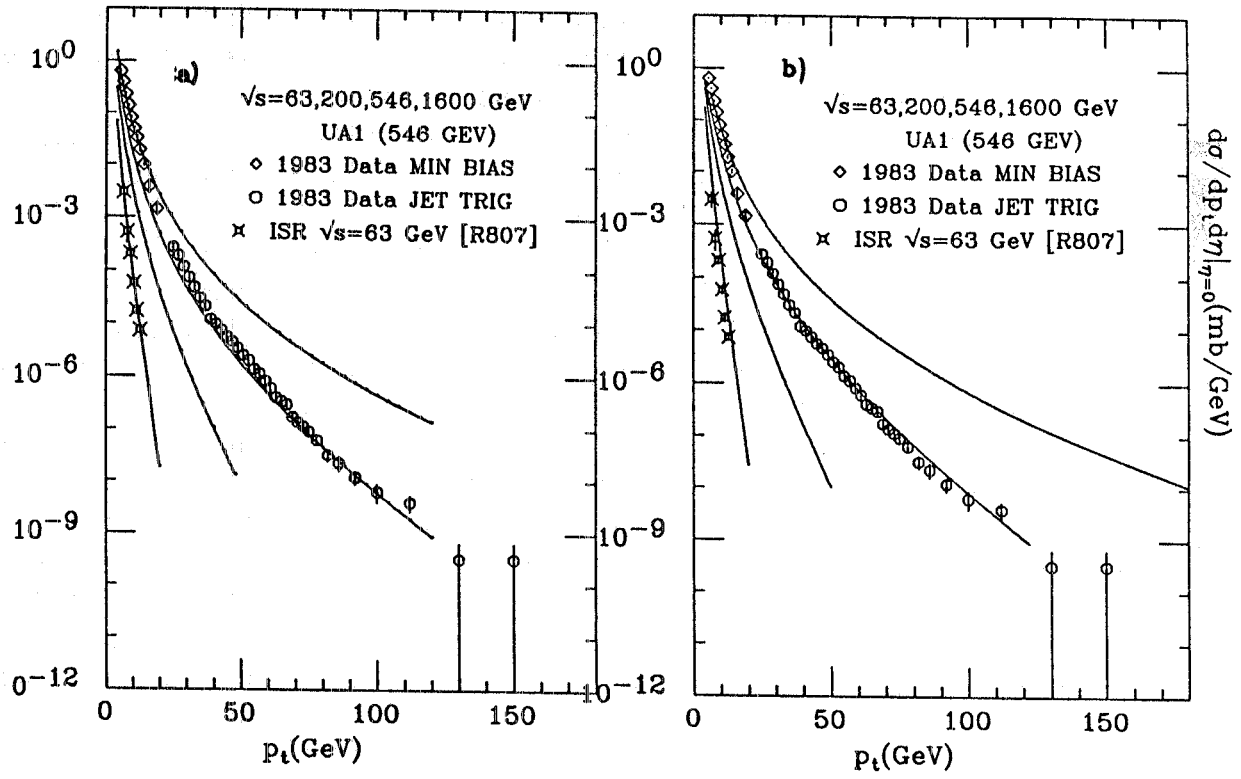

Fig.2 : Theoretical curves for $\frac{d\sigma}{dp_t d\eta}|_{\eta=0}$ vs. p_t obtained through Eq.(1) for $\sqrt{s} = 63, 200, 546$ and 1600 GeV using Duke and Owens densities with $Q^2 = p_t^2$, $N_f = 5$, mode 1 (ref. 17) in (a) and EHLQ densities with $Q^2 = \frac{p_t^2}{4}$ $N_f = 4$, mode 2 (ref.18) in (b). 63 GeV data are from ref.19,experiment R807. 546 GeV data are from ref. 20 (○ UA1 1983 Data from Jet Trigger) and ref.13 (◇ UA1 1983 Data from minimum bias).

$$|A|^2 = \frac{9}{8}\frac{(3+z^{*2})^3}{(1-z^{*2})^2} \qquad (2b)$$

In Eq.(2) the non-singular proton structure function F(x) is defined as

$$F(x) = G(x) + \frac{4}{9}\left(Q(x) + \bar{Q}(x)\right)$$

with G(x), Q(x) and $\bar{Q}(x)$representing the density of gluons, quarks and antiquarks, respectively. For a comparison we show the calculation for two different choices of parton densities, Duke and Owens in mode 1 [17] and EHLQ in mode 2 [18]. ISR[19] and S$\bar{p}$pS data [13,20] shown in **Fig.2a** indicate that, while the agreement with experiments is good at ISR, a multiplicative, energy-dependent K-factor is needed at the Collider. Such a factor is attributed to the presence of higher order QCD corrections. Following the suggestion by EHLQ, one can try to minimize these corrections by an appropriate choice of the scale, for instance $Q^2 = \frac{p_t^2}{4}$. This is shown in **Fig.2b** where the QCD prediction is obtained using EHLQ parton densities. Unfortunately one notices that while the agreement with high energy data has slightly improved at high E_T, this choice of scale does not reproduce the ISR data as well as the previous choice. Moreover the low-E_T jet cross-section at the collider still lies higher than the QCD curve indicating the need for more precise corrections in the region where α_s is large. A likely source of corrections is initial state radiation (soft gluon

bremsstrahlung) which would change the kinematics in a region where the cross-section is rapidly varying. While this problem will require a complete investigation, in the following we shall concentrate on the first order QCD calculation of integrated jet yields.

Differences between the choices of scale (Q^2) are more evident in the low p_t region. This is the dominant region in the calculation of the integrated jet cross-section (as discussed later) and also the region recently investigated by the UA1 group. UA1 has reported observation of the jet phenomenon down to transverse energies of a few GeV[13]. These jets, which occur in the jet energy domain of the ISR, experimentally are an entirely new phenomenon with respect to the high E_T jets previously reported by UA1 and UA2. The rate of these events at a given E_T is a very fast growing function of $\sqrt{s}$. On the other hand, if one integrates in p_t, the rate of increase with energy of the jet yield depends crucially on the lowest p_t of the jets, p_0 and on the rapidity cuts. To show this we calculate the jet yield at different energies, in the central region, $|\eta| < 1.5$ for various rapidity values, integrating Eq.(2) in p_t from minimum values $p_0 = 3,4\ GeV$. The curves shown in **Fig.3** indicate that the widening of the rapidity plateau is accompanied by the general QCD result that as the energy increases, more and more jets are produced in the central region.

We now consider the partially integrated cross-section for $|\eta| < 1.5$ and for p_0=3,4 GeV. We give the results of this calculation in **Fig.4**. It is instructive to compare these

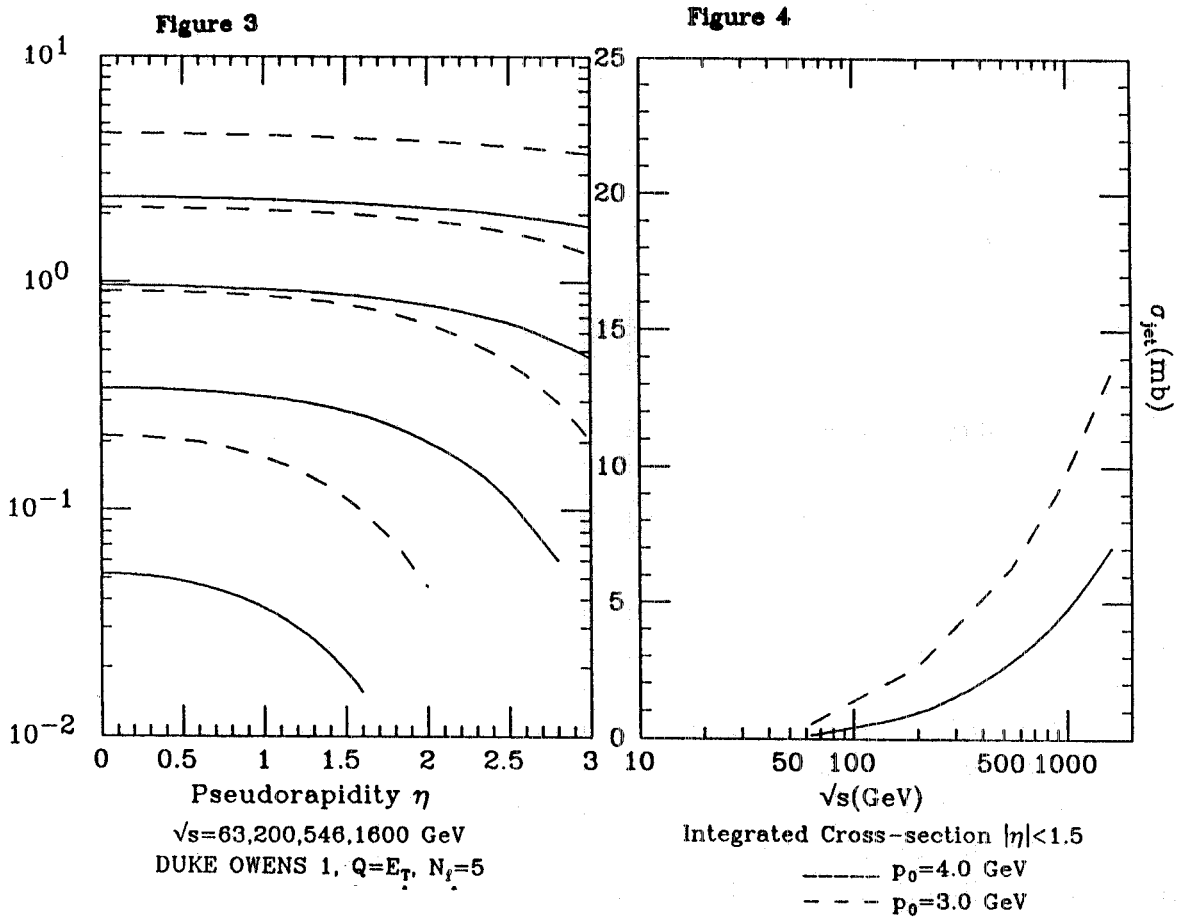

Fig.3 : $\frac{d\sigma_{jet}}{d\eta}$ vs η in the central region, using Duke and Owens densities, mode 1, Q=p_t, N_f=5, p_0=3 and 4 GeV respectively.

Fig.4 : σ_{jet} vs. $\sqrt{s}$ is shown after integrating Eq.(2) using Duke and Owens densities as in fig. 2a, $p_0 = 3,4\ GeV$ and $|\eta| < 1.5$.

rates with the rate of increase of the inelastic cross-section, which we take to be $\frac{2}{3}\sigma_{tot}$ and for σ_{tot} we use the parametrization given by U.Amaldi et al. We find that the jet yield, in the central region, at the Cern Collider varies from a minimum fraction of 0.027 at $\sqrt{s} = 200\ GeV$ to a maximum of 0.096at $\sqrt{s} = 900\ GeV$, for $p_0 = 4\ GeV$.

The rate of increase is more dramatic if one calculates the jet yield in the full rapidity range, where sizable violations of KNO scaling have been observed by the UA5 collaboration. We shall dedicate the next section to the discussion of the total jet cross-section.

3. - THE INTEGRATED JET CROSS-SECTION

In this section we calculate the fully integrated 2-jet cross section for various approximations, different densities and various choices of the QCD scale Q^2, and compare the results with UA1 data. This comparison will help clarify the dependence of the threshold parameter p_0 from the above choices. One implicit dependence, which we do not specifically take into account, is that coming from the K-factor. Since the latter is energy dependent, an accurate determination of p_0 can only be done when the absolute normalization of the QCD cross-section will be fully clarified. For K=1, the result of our calculations indicate that a value of 5 GeV for p_0 is much too low to account for the UA1 results, even if one takes everything in one's favour, for instance by choosing $Q^2 = \frac{p_0^2}{4}$. We shall return to discuss this point later in this section.

To calculate the fully integrated jet yield, one can integrate eq.(2) or use an alternative expression, which expresses the 2-jet differential cross-section through the parton-parton center of mass scattering angle,i.e.

$$\sigma_{jet}(s) = \frac{1}{2}\int dx_1 \int dx_2 \int d\cos\theta^* \frac{d\sigma}{dx_1 dx_2 d\cos\theta^*}$$

In the dominant small angle limit, one can write

$$\frac{d\sigma}{dx_1 dx_2 d\cos\theta^*} = \frac{9\pi[\alpha_s(Q^2)]^2}{32s}\frac{F(x_1,Q^2)}{x_1^2}\frac{F(x_2,Q^2)}{x_2^2}\frac{(3+\cos\theta^{*2})^3}{(1-cos\theta^{*2})^2} \qquad (3)$$

where θ^* is the scattering angle in the center of mass of the parton-parton system and the integration in $\cos\theta^*$ extends between $-z_0$ and $+z_0$ with

$$z_0 = \sqrt{1 - \frac{4{p_0}^2}{sx_1x_2}}$$

The calculation of the jet yield is numerically simplified if one neglects the angular dependence in $\alpha_s(Q^2)$. Then the integration in $\cos\theta^*$ is straightforward and gives

$$\int d\cos\theta^* \frac{d\sigma}{dx_1 dx_2 d\cos\theta^*} = \frac{9\pi}{16s}\frac{F(x_1,Q^2)}{{x_1}^2}\frac{F(x_2,Q^2)}{{x_2}^2}\left[\alpha_s(Q^2)\right]^2 I(p_0) \qquad (4)$$

with

$$I(p_0) = \frac{8sx_1x_2}{{p_0}^2}\sqrt{1-\frac{4p_0^2}{sx_1x_2}} - 16ln\frac{1+\sqrt{1-\frac{4p_0^2}{sx_1x_2}}}{1-\sqrt{1-\frac{4p_0^2}{sx_1x_2}}} + \sqrt{1-\frac{4p_0^2}{sx_1x_2}}\left(\frac{34}{3} - \frac{4}{3}\frac{{p_0}^2}{sx_1x_2}\right) \quad (5)$$

A further simplification is obtained if one neglects ,in eq.(5), terms of higher order in $\frac{4{p_0}^2}{sx_1x_2}$. One can then write[21)]

$$\sigma_{2-jets}(s) = \frac{9\pi}{2{p_0}^2}\int_\epsilon^1 \frac{dz}{z}F(\frac{\epsilon}{z},Q^2)\int_x^1 \frac{dx}{x}F(x,Q^2)\left[\alpha_s(Q^2)\right]^2 \quad (6)$$

with $\epsilon = \frac{4p_0^2}{s}$. To study how reliable this approximation is at present energies, we have compared the total 2-jet yield obtained using the complete expression, eqs.(4)and (5), with the approximate form given by eq.(6). In either case,we have used UA1 parametrization for parton densities i.e.

$$F(x) = 6.2e^{-9.5x} \quad (7)$$

and an integration cutoff $p_0 = 5GeV$. Also, we have chosen for the argument of α_s the quantity $Q^2 = \frac{p_0^2}{4}$. As one can see from **Fig.5** the two calculations give different results,

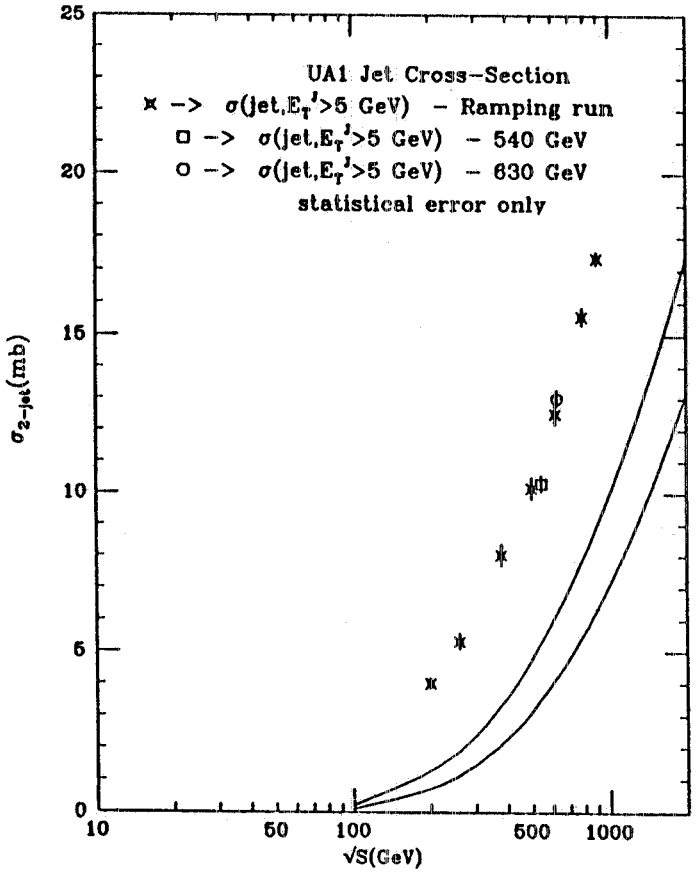

Fig.5 : σ_{jet} vs. $\sqrt{s}$ for $p_0 = 5\ GeV$, $\alpha_s(\frac{p_0^2}{4})$ using UA1 densities. Upper curve refers to the approximate expression, eq.(6), lower curve uses eq.(5).

even though, as the energy increases, the ratio $\frac{\Delta\sigma}{\sigma}$ decreases a as one naively expects. From this figure it appears that :

(i) while approximation (6) may be viable at higher energies it is preferable not to use it in the energy range available by the Cern Collider;

(ii) cut-offs as low as 5 GeV do not give large enough cross- sections at $\sqrt{s} = 546GeV$ to account for various anomalies discussed at the beginning.

Comparing this with the low-p_t jet yield as measured by UA1 for a nominal jet threshold at 5 GeV[13] , one concludes that the effective cut-off must be lower than the "declared" value. This is partly due to the presence of the underlying event which contributes, more or less isotropically to the measurement of all the transverse energy deposited in the calorimeters. Thus a jet event can be produced from a 3 GeV parton together with $\approx 2 \div 3$GeV of soft debris from the underlying event.

Above considerations leave a large degree of arbitrariness in the calculation of the jet yield. To reduce some of the uncertainties we shall in the following discuss various choices of densities and parameters and how they affect the calculation of the 2-2 jet cross- section.

We first calculate the cross-section using UA1 parton densities and for the following four choices for the QCD scale :

(a) $Q^2 = \frac{{p_0}^2}{4}$

(b) $Q^2 = \frac{p_t^2}{4}$

(c) $Q^2 = \frac{sx_1x_2}{16}$

(d) $Q^2 = sx_1x_2$

In **Fig.6** we show the comparative cross-sections for the above four different QCD scale choices and $p_0 = 3$ and 4 GeV. One notices that :

(i) to keep the angular dependence in α_s (case b) or to evaluate the latter at the smallest possible p_t value (case a) give very similar results,

(ii) the cross-section grows less rapidly with energy if the scale is proportional to s as in cases c) and d).

The above calculations are based on densities measured in a limited energy range. The use of this set is numerically convenient but not justified outside the energy range of the Cern Collider. To show the effect of the evolution of the parton densities on the calculation of the jet yield, we show in **Fig.7** the cross-section with UA1 densities and with EHLQ parametrization, mode 2, $Q^2 = sx_1x_2$. As expected, at higher energies, the densities from ref.18,being more peaked at smaller x values, give a larger contribution. Notice that the choice $Q^2 = sx_1x_2$ requires a threshold value $p_0 < 3GeV$ to account for the data.

So far, the analysis of low E_T jets in minimum bias events shows a sharp rise with energy in the contribution to the inelastic cross- section. This experimental observation is in agreement with the numerical estimates of the quantity σ_{2-jets} as obtained from first order QCD calculations. However at even higher energis to be reached by TeV I, LHC and SSC, values of x as small as $\approx 10^{-4}$ contribute significantly to the cross-section with $p_0 \approx 5 \div 10$GeV. For such small x values, the parton densities would become large enough to make multiple, independent parton-parton collisions a sizable contribution to the inelastic cross-section. Indeed these terms, which are of higher order in α_s, become important as the parton luminosity increases with energy for any fixed p_0 of the partons. Some evidence for multiple jet production may already be available at the Cern S$\bar{p}$pS from both UA1 and UA2 groups. We shall briefly discuss this point in the next section.

Figure 6

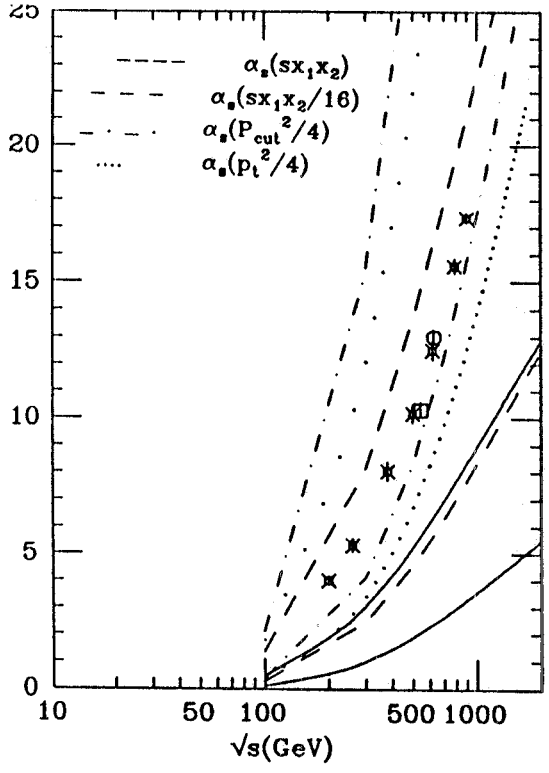

Figure 7

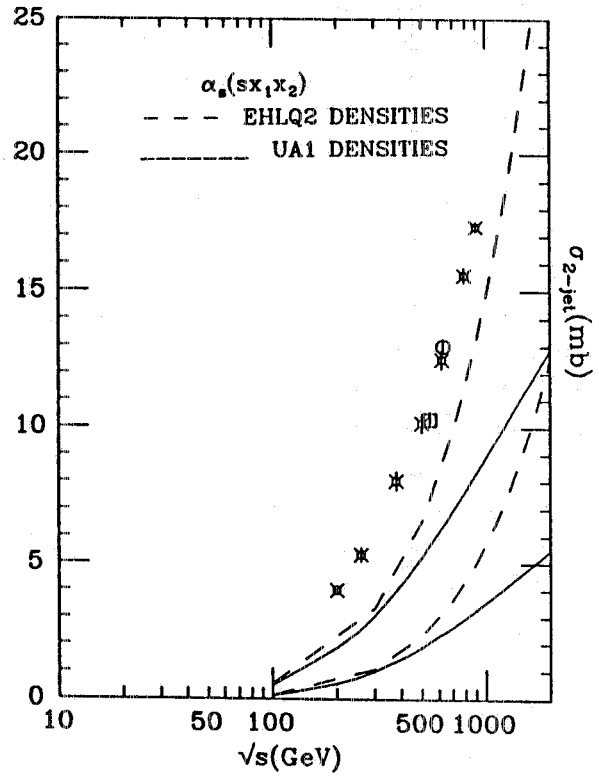

Fig. 6 : σ_{jet} vs. $\sqrt{s}$ using UA1 densities for various $\alpha_s(Q^2)$:
$Q^2 = sx_1x_2$, continuous line;
$Q^2 = \frac{1}{16}sx_1x_2$, dashed line;
$Q^2 = \frac{p_t^2}{4}$, dotted line ;
$Q^2 = \frac{p_0^2}{4}$, dash-dotted line.
For each type of line, the upper and lower curves refer to $p_0 = 3$ and 4 GeV respectively. Data shown are from ref. 13 and represent preliminary UA1 data taken during the Ramping Run ($\diamond$) as well as during 1983 ($\sqrt{s} = 546$ GeV) and 1984 ($\sqrt{s} = 630$ GeV).

Fig.7 : σ_{jet} vs. $\sqrt{s}$ using EHLQ densities, mode 2 (continuous line) and UA1 densities (dashed lines). The upper two curves are for $p_0 = 3$ GeV and the lower two for $p_0 = 4$ GeV, $\alpha_s(sx_1x_2)$. Data are the same as in fig.6.

4. - MULTIPARTON COLLISIONS

The 4-jet yield due to 2 independent parton-parton scattering processes is approximately given by[18,22,23]

$$\frac{d\sigma_4}{dE_T} \approx \int_{p_0}^{E_T-p_0} dE_1 \int_{p_0}^{E_T-p_0} dE_2 \frac{d\sigma_2}{dE_1}\frac{d\sigma_2}{dE_2}\frac{1}{\sigma_{tot}}\delta(E_T - E_1 - E_2) \qquad (8)$$

where $\frac{d\sigma_2}{dE}$ is the 2-2 parton cross-section folded with the parton densities and integrated over the rapidity variable. Upon integration over the transverse energy variable, eq.(8) can be further simplified to read[22)]

$$\frac{\sigma_4}{\sigma_{tot}} \approx \frac{1}{2}(\frac{\sigma_2}{\sigma_{tot}})^2 \tag{9}$$

We have seen that the ratio $\frac{\sigma_2}{\sigma_{tot}}$ increases with energy in the present energy range. Eq.(9) then indicates that also the ratio $\frac{\sigma_4}{\sigma_2}$ would increase. This implies the presence of a small, but finite fraction of multiple parton scattering events already at the CERN Collider. From the measured jet fraction as reported by UA1[13)], we can obtain the values indicated in Table I.

Table I

$\sqrt{s}$ GeV	$\frac{\sigma_j}{\sigma_t}$	$\frac{\sigma_2}{\sigma_t}$	$\frac{\sigma_4}{\sigma_2}$	$\frac{\sigma_4}{\sigma_t}$
200	0.076	0.074	0.037	0.0027
500	0.166	0.154	0.077	0.012
900	0.254	0.228	0.114	0.025

An extrapolation of these results to $\sqrt{s}$ =2 TeV gives for $\sigma_4 \approx 3 \div 4mb$, for a nominal jet detection threshold at 5 GeV. This is probably an overestimate, but it reflects the general problem of properly taking into account the contribution coming from multiple parton scattering. The above expression is obtained in the limit in which one neglects all the correlations between partons emitted by the same hadron. An improved formula would take into account longitudinal and transverse momentum constraints.

Such independent multiple parton scattering effects will also manifest themselves in the KNO function at higher energies. Just like violations of KNO scaling at the Collider have revealed the presence of a large number of hard scattering events in the inelastic cross-section, similarly a further widening of the distribution may signal the presence of a rising contribution from multiple parton processes. Indeed, if $\Psi(\frac{n}{<n>})$ keeps flattening as presently indicated by UA5 results[24)] - through the Tevatron and beyond - multiple parton collisions may be the reason. In this respect, our 2-component model for KNO scaling violations

$$\sigma_{n\ ch} = \sigma^{(0)}_{n\ ch} + \sigma^{(1)}_{n\ ch} \tag{10}$$

was only a first step. With $\frac{<n>_0}{<n>_1}$ fixed and Ψ_0 and Ψ_1 scaling, one does not obtain an indefinite flattening of the total KNO function, but only a shift from one Ψ to the other, as the relative weight increases. On the other hand this may very well be what would happen in the limit of an indefinite number of independent particle production processes, each of them characterized by an increasing average charged multiplicity. This problem is at present under investigation and the results will be presented elsewhere.

5. - CONCLUSIONS

To summarize, we have analyzed in some detail the production of low-E_T jets in minimum bias events at present energies (60 ÷ 1600 GeV), to probe the uncertainties introduced by the choice of Q^2, the K- factor, parton densities at small x and a rather crucial critical dependence on p_0. Despite these difficulties, it seems safe to conclude that a large fraction of the inelastic data at high energies can indeed be understood in terms of low-E_T jets, with a transverse momentum threshold lower than 5 GeV and larger than 2 GeV. The threshold value is strongly affected by the choice of QCD scale and the K-factor. For $Q^2 = \frac{p_T^2}{4}$ and K=1, we find $p_0 \approx 3.5 GeV$ in the energy range of the collider. Beyond present energies, hard multiple collisions begin to play a non-negligible role and must be included in any quantitative estimate of the inelastic cross-section as well as the KNO function. If these phenomenological observations are borne out at the Tevatron, an important theoretical effort should be done to discover a dynamical mechanism which would free a calculation of σ_{tot} from p_0 and yet not significantly alter the differential transverse momentum distributions.

ACKNOWLEDGMENTS

We have benefited from many useful discussions with G.Ciapetti, T.Gaisser, N.Paver and D.Treleani. We also thank C.Rubbia for his interest and continuous advice on this problem.

REFERENCES

(1) G.Arnison et al., Physics Letters 118*B*, 167(1982).UA1 Collaboration.
(2) C.M.G. Lattes et al., Physics Reports 65, 151 (1980).
(3) A. Breakstone et al.,Physical Review *D*30, 528 (1984). ABCDHW Collaboration.
(4) G.Alpgard et al.,Physics Letters 121*B*, 209 (1983). UA5 Collaboration.
G.Alner et al., Physics Letters 138*B*,304(1984). UA5 Collaboration.
(5) For a recent review of elastic and total cross-section data, see : R.Castaldi and G.Sanguinetti, Annual Review of Nuclear and Particle Science 35, 351 (1985).
(6) G.Pancheri and C.Rubbia, Nuclear Physics *A*418,117c (1984).
(7) G.Pancheri, Y.Srivastava and M.Pallotta, Phys. Letters 151*B*, 453 (1985).
(7) G.Pancheri and Y.Srivastava, Physics Letters 159*B*, 69 (1985).
(8) D.Cline, F.Halzen and J.Luthe, Physical Review Letters 31, 491 (1973).
(9) T.K.Gaisser and F.Halzen, Physical Review Letters 54,1754(1985).
(10) L.V.Gribov, E.M.Levin and M.G.Ryskin, Physics Reports 100, 1 (1983).

(11) M. Albrow et al., Nuclear Physics *B*118, 1 (1976).
J.C.M. Armitage et al., Nuclear Physics *B*194, 365 (1982).
M.Bozzo et al.,Physics Letters 136*B*,217 (1984).
(12) U.Amaldi et al., Physics Letters 66*B*,390 (1977).
(13) G.Ciapetti, Proceedings of the 5th Topical Workshop on Proton-Antiproton Collider Physics, Saint-Vincent, Aosta Valley, 25 February-1 March 1985. Ed. by M.Greco.
F.Ceradini, Proceedings of the International Europhysics Conference on High Energy Physics, Bari,Italy 18-24 July 1985. Ed. by L.Nitti and G.Preparata.
F.LaCava, Presented at the VI Topical Workshop on Proton- Antiproton Collision, Aachen, June 30-July 3rd 1986.
(14) R.Horgan and M.Jacob, Nuclear Physics *B*179, 441 (1981).
(15) M.Banner et al., Physics Letters 118*B*, 203 (1982). UA2 Collaboration.
G.Arnison et al., Physics Letters 123*B*, 115 (1983). UA1 Collaboration.
P.Bagnaia et al.,Physics Letters 138*B*,430 (1984).UA2 Collaboration.
J.Appel et al.,Physics Letters 160*B*,349 (1984). UA2 Collaboration.
G.Arnison et al.,Physics Letters 132*B* 214 (1984). UA1 Collaboration.
L.Di Lella, Annual Review of Nuclear and Particle Science 35, 107 (1985),
(16) G.Arnison et al., Physics Letters 136*B*, 294 (1984).
(17) D.W.Duke and J.F.Owens, Physicsl Review *D*30, 49 (1984).
(18) E.Eichten, I.Hinchliffe, K.Lane and C.Quigg, Review of Modern Physics 56, 579 (1984).
(19) C.Bromberg et al., Physical Review Letters 43, 565 (1979).
M.D. Corcoran et al., Physical Review Letters *underline*44, 514 (1980).
(20) G.Arnison et al.,Physics Letters 172*B*, 461 (1986).
(21) A.H. Mueller, Proceedings of the APS/DPF Meeting, Eugene Oregon, August 12-15, 1985.
(22) N.Paver and D.Treleani, Physics Letters 146*B*, 252 (1984); Zeit Physics *C*28,187 (1985); Proceedings of the APS/DPF Meeting, Eugene Oregon, August 12-15, 1985.
(23) M.Jacob, Cern-TH-3693(1983).
P.V.Landshoff anf J.Polkinghorne, Physical Review *D*18, 3344 (1978).
B.Humpert,Physics Letters 131*B*,461 (1983).
(24) G.J.Alner et al.,CERN-EP/85-62. UA5 Collaboration.
J.G. Rushbrooke, Proceedings of the International Europhysics Conference on High Energy Physics, Bari,Italy 18-24 July 1985. Ed. by L.Nitti and G.Preparata.